

1,2-Azolyamidino Ruthenium(II) Complexes with dmsO Ligands:  
Electro- and Photocatalysts for CO<sub>2</sub> ReductionReceived 00th January 20xx,  
Accepted 00th January 20xx

DOI: 10.1039/x0xx00000x

Murphy Jennings,<sup>a</sup> Elena Cuéllar,<sup>b</sup> Ariadna Rojo,<sup>b</sup> Sergio Ferrero,<sup>b</sup> Gabriel García-Herbosa,<sup>c</sup> John Nganga,<sup>d</sup> Alfredo M. Angeles-Boza,<sup>a,d</sup> Jose M. Martín-Alvarez,<sup>b</sup> Daniel Miguel,<sup>b</sup> and Fernando Villafañe\*<sup>b</sup>

New 1,2-azolyamidino complexes *fac*-[RuCl(dmsO)<sub>3</sub>(NH=C(R)az<sup>\*</sup>-*κ*<sup>2</sup>N,N)]OTf [R = Me (**2**), Ph (**3**); az<sup>\*</sup> = pz (pyrazolyl, **a**), indz (indazolyl, **b**)] are synthesized via chloride abstraction from their corresponding precursors *cis, fac*-[RuCl<sub>2</sub>(dmsO)<sub>3</sub>(az<sup>\*</sup>H)] (**1**) after a subsequent base-catalyzed coupling of the appropriate nitrile with the 1,2-azole previously coordinated. All the compounds are characterized by <sup>1</sup>H, <sup>13</sup>C NMR and by IR. Those derived from MeCN are also characterized by X-Ray diffraction. Electrochemical studies showed several reduction waves in the range -1.5 to -3 V. The electrochemical behavior in CO<sub>2</sub> media is consistent with CO<sub>2</sub> electrocatalyzed reduction. The catalytic activity expressed as [*i*<sub>cat</sub>(CO<sub>2</sub>)/*i*<sub>p</sub>(Ar)] ranged from 1.7 to 3.7 for the 1,2-azolyamidino complexes at voltages of *ca.* -2.7 to -3 V vs. ferrocene/ferrocenium. Controlled potential electrolysis showed rapid decomposition of the Ru catalysts. Photocatalytic CO<sub>2</sub> reduction experiments by compounds **1b**, **2b** and **3b** carried out in a CO<sub>2</sub>-saturated MeCN/TEOA (4:1 v/v) solution containing a mixture of the catalyst and [Ru(bipy)<sub>3</sub>]<sup>2+</sup> as the photosensitizer under continuous irradiation (light intensity of 150 mW/cm<sup>2</sup> at 25 °C, λ > 300 nm) show that compounds **1b**, **2b** and **3b** allowed CO<sub>2</sub> reduction catalysis, producing CO and trace amounts of formate. The combined turnover numbers for the production of formate and CO is *ca.* 100 after 8 h and follows the order **1b** < **2b** ≈ **3b**.

## Introduction

Research on the catalytic reduction of CO<sub>2</sub> is receiving an intense attention, since it is a key component to a sustainable future. A variety of transition metal complexes have been reported to display electrochemical CO<sub>2</sub> reduction activities, however, novel catalytic systems are still required to cope with the social dilemma of climate change.<sup>1</sup> Ruthenium(II) complexes are among those more studied, and in fact the electrochemical CO<sub>2</sub> reduction catalyzed by *cis*-[Ru(bipy)<sub>2</sub>(CO)<sub>2</sub>]<sup>2+</sup> (bipy = 2,2'-bipyridine) and *cis*-[Ru(bipy)<sub>2</sub>(CO)Cl]<sup>+</sup> were among the first systems reported, back in 1987.<sup>2</sup> Since then, a plethora of Ru catalysts have been described in the context of CO<sub>2</sub>

electroreduction, most of them containing two bipy ligands coordinated *cis*, or other polypyridine type ligands with similar geometries.<sup>1-3</sup> The use of mono(bipy) complexes is limited to carbonyl complexes such as [Ru(N-N)(CO)<sub>2</sub>Cl<sub>2</sub>], (N-N = bipy or substituted bipy), or cationic derivatives derived from the substitution of the chlorido by neutral ligands, and to their corresponding reduced Ru(0) species.<sup>4</sup>

Reduction of carbon dioxide can also be achieved by photochemical methods. The catalysts for these processes are usually metal complexes with different accessible redox states available in both the central metal and in the ligands in order to drive the multi-electron reduction process for CO<sub>2</sub> reduction.<sup>5</sup> In the case of Ru(II), both bis(bipy)<sup>6</sup> and mono(bipy)<sup>7</sup> complexes have been widely studied as photocatalysts for CO<sub>2</sub> reduction to give CO and/or formate, depending on the reaction conditions.

The activity of the catalyst largely depends on the substituents of the ligands which are key factors on both the primary coordination sphere of the transition metal center, and also on the secondary coordination effects. The latter has been taken into consideration only very recently, when the first reports on the role of pendant groups which may lead to supramolecular arrangements has been described.<sup>8</sup> However, synthetic methods for substituted bipy ligands are usually difficult and/or tiresome, and thus the alternative of coupling two monodentate ligands to afford a chelating diimine ligand appears as a straightforward method in order to obtain N,N-chelating ligands by accessible synthetic paths.<sup>9</sup> 1,2-azolyamidino ligands fulfill these requirements, as they can be easily obtained *in situ* by the coupling reaction of 1,2-azoles and coordinated nitriles (Scheme 1). We have exploited this

<sup>a</sup> Institute of Materials Science, University of Connecticut, 97 N. Eagleville Rd, Storrs, CT 06269, USA.

<sup>b</sup> GIR MIOMeT-IU Química-Química Inorgánica, Facultad de Ciencias, Campus Miguel Delibes, Universidad de Valladolid, 47011 Valladolid, Spain. E-mail: fernando.villafane@uva.es

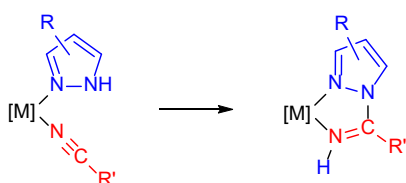
<sup>c</sup> Departamento de Química, Facultad de Ciencias, Universidad de Burgos, 09001 Burgos, Spain.

<sup>d</sup> Department of Chemistry, University of Connecticut, 55 N. Eagleville Rd, Storrs, CT 06269, USA.

† Footnotes relating to the title and/or authors should appear here.

Electronic Supplementary Information (ESI) available: [Cyclic Voltammograms of complexes **1-3**, solution stability tests, TEM of **2b** degradation products, turnover numbers for the production of H<sub>2</sub>, CO, and HCCOH at different times for compounds **1b**, **2b**, and **3b**, isotope labeling experiments for clarifying off carbon source of CO production, <sup>1</sup>H NMR spectra of complexes **1-3**. CCDC 2221963-2221964 contain the supplementary crystallographic data for this paper (crystal structures of complexes **2a** and **2b**). These data can be obtained free of charge via www.ccdc.cam.ac.uk/data\_request/cif, or by emailing data\_request@ccdc.cam.ac.uk, or by contacting The Cambridge Crystallographic Data Centre, 12 Union Road, Cambridge CB2 1EZ, UK; fax: +44 1223 336033. See DOI: 10.1039/x0xx00000x

reaction, i.e. the metal-mediated coupling of 1,2-azoles and nitriles, so a wide range of new 1,2-azolyamidino complexes can be thus easily obtained.<sup>10</sup> The use of different 1,2-azoles and nitriles provides the opportunity of controlling the main features, electronic and steric, of the ligand. In particular, the electrochemical and luminescent properties, of Re(I)-tricarbonyl and cis-bis(bipyridyl)Ru(II) complexes containing 1,2-azolyamidino ligands have been reported, as well as the photocatalytic behaviour of the latter.<sup>11</sup> The same reaction using a nucleobase such as 1-methylcytosine instead of the 1,2-azole has revealed to be a new method to incorporate of biologically relevant substrates into Re(I) tricarbonyl complexes.<sup>12</sup>



**Scheme 1** Synthesis of a 1,2-azolyamidino ligand from the (1,2-azole) precursor containing a coordinated nitrile.

Another aspect of interest on the 1,2-azolyamidino ligands lays on the presence of an acidic NH group, which allow further significant reactivity, as it may be involved in noncovalent interactions. A relevant example is the ability of the *fac*-[Re(CO)<sub>3</sub>(Hdmpz)(HN=C(Me)dmpz-κ<sup>2</sup>N,N)]<sup>+</sup> cation to bind selectively chloride anions by combining electrostatic attraction and hydrogen bonding of the NH groups present.<sup>13</sup> A second exponent, this time on Mn(I), emerges from the use of a somehow uncommon nitrile, such as dicyanamide, which allowed to obtain a bimetallic Mn(I) complex containing a bridging tetradentate bis(pyrazolylamidino) ligand, where the bromide anion plays an crucial role on its planarity, as demonstrated by DFT calculations.<sup>14</sup>

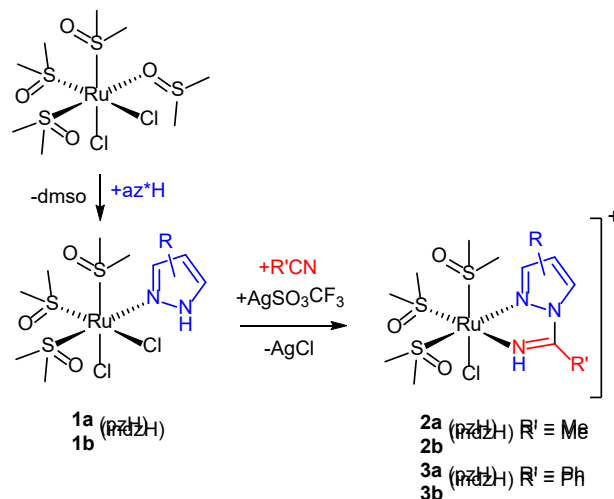
Herein we report the synthesis and characterization of new 1,2-azolyamidino Ru(II) complexes. Their chlorido(1,2-azole) precursors are also described. The 1,2-azoles used in this work are pyrazole (pzH) and indazole (indzH), whereas the nitriles are acetonitrile (MeCN) and benzonitrile (PhCN). This allows to study easily obtained 1,2-azolyamidino ligands with different electronic and steric properties. The behavior of the complexes synthesized as electro- and photocatalysts for the reduction of CO<sub>2</sub> is described.

## Results and discussion

### Synthesis and characterization of the complexes

The synthesis of the complexes described in this work is depicted in Scheme 2. A panel of complexes with different substituents were synthesized in order to confirm the synthetic method and to study the influence of the substituents on the electrocatalytic reduction of CO<sub>2</sub>. Scheme 2 includes the mixed chlorido(1,2-azole) complexes *cis, fac*-[RuCl<sub>2</sub>(dmsO)<sub>3</sub>(az\*H)] (**1**) (az\* = pz, indz), which are precursors of the 1,2-azolyamidino *fac*-[RuCl(dmsO)<sub>3</sub>(NH=C(R)az\*-κ<sup>2</sup>N,N)]OTf (R = Me, Ph)

complexes, as a result of coupling of a coordinated pyrazole (pzH) or indazole (indzH) in **1** with acetonitrile (R = Me, **2**) or benzonitrile (R = Ph, **3**) (Scheme 1). Complexes **1a** and **1b** had been previously reported by Ferrer *et al.*<sup>15</sup> and by Reisner *et al.*<sup>16</sup> respectively. Herein we report a new synthetic procedure and their thorough characterization.



**Scheme 2** Synthesis of the new complexes. .

Chlorido(1,2-azole) complexes **1a** and **1b** were obtained by substituting the O-coordinated DMSO ligand in the parent complex *cis*-[RuCl<sub>2</sub>(dmsO)<sub>4</sub>] by pyrazole or indazole, respectively (Scheme 2). These synthetic methods have been improved compared to those previously described in the literature. Thus, the pyrazole complex (**1a**) is herein obtained at room temperature, whereas Ferrer *et al.*<sup>15</sup> used refluxing methanol. Moreover, our reaction leading to the indazole complex **1b** lasts one hour at room temperature, whereas Reisner *et al.*<sup>16</sup> reported an overnight reaction. The 1,2-azolyamidino complexes **2** and **3** were obtained by extracting with silver triflate one of the chlorido ligands in presence of the nitrile, followed by the coupling of nitrile and the 1,2-azole using NaOH (aq.) as catalyst, as we have previously described.<sup>10c</sup>

The spectroscopic data are straightforward and support the proposed geometries (see Experimental section). Complexes **2a** and **2b** were also characterized by single-crystal X-ray diffraction studies (Fig. 1). The distances and angles (CCDC 2221963–2221964) are similar to those found in other Ru(II) similar ligands.<sup>17</sup> Thus, the C(4)–N(3) distances (1.265(4) Å and 1.279(4) Å respectively for **2a** and **2b**) are typical of C=N double bonds. In complexes **2a** and **2b** the N-bound hydrogens of the 1,2-azolyamidino ligands are involved in hydrogen bonding with an oxygen atom of a triflate anion. The distances and angles detected for **2a** (H(3)⋯O(4) 2.050 Å, N(3)⋯O(4) 2.885 Å, N(3)–H(3)⋯O(4) 163.4°) and **2b** (H(3)⋯O(4) 2.006 Å, N(3)⋯O(4) 2.840 Å, N(3)–H(3)⋯O(4) 162.8°) may be considered as “moderate” hydrogen bonds.<sup>18</sup>

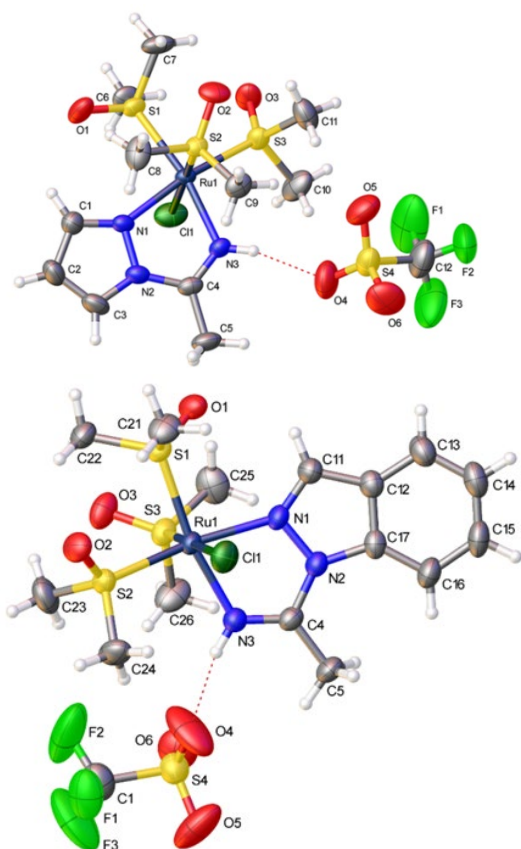


**Figure 1** Perspective views of *fac*-[RuCl(dmsO)<sub>3</sub>(NH=C(Me)pz- $\kappa^2$ N,N)](OTf), **2a**, (above) and *fac*-[RuCl(dmsO)<sub>3</sub>(NH=C(Me)indz- $\kappa^2$ N,N)](OTf), **2b**, (below) showing the atom numbering. Thermal ellipsoids are drawn at 50% probability.

### Electrochemical studies

Table 1 gathers the observed potential values obtained from cyclic voltammetry (CV) experiments, referenced to the redox pair ferrocenium/ferrocene, following the IUPAC recommendations.<sup>19</sup> A AgCl/Ag (3M NaCl) reference electrode was used, and ferrocene was added as internal calibrant always in the last experimental measurement. All the measurements were made in MeCN, once the stability of the complexes in this solvent was confirmed by NMR.

Scanning to negative potentials under N<sub>2</sub>, all the complexes display several waves, as the result of successive electron transfer reductions. This is probably the result of the pyrazolylamidino ligand reduction, as occurs in Ru<sup>II</sup>(bipy) systems, which display one or several waves at negative potentials, which have been always assigned to bipy-based reductions.<sup>3b,6f</sup> When the same scans were carried out under CO<sub>2</sub> atmosphere, the indazole complexes and the pyrazole complex **2a** showed a clear enhancement of the cathodic current (red lines in Figs. S1, ESI). This electrochemical behaviour is consistent with CO<sub>2</sub> activation, i. e. electrocatalyzed reduction. The ratio  $i_{cat}(CO_2)/i_p(N_2)$  allows comparing the electrochemical activity of the complexes, with values ranging from 1.7 to 3.7 for the 1,2-azolylamidino complexes (Table 1). As a representative example, the results registered for the complex *fac*-[RuCl(dmsO)<sub>3</sub>(NH=C(Ph)indz-

$\kappa^2$ N,N)](OTf) (**3b**) are shown in Fig. 2. Black (N<sub>2</sub>) and red (CO<sub>2</sub>) traces overlap completely in the range -1.25 to 0.0V. Changing the atmosphere from N<sub>2</sub> to CO<sub>2</sub> generates a great enhancement of the current at potentials below -2.5V. The rest of the experiments under CO<sub>2</sub> atmosphere lead to different shapes of the waves associated to electrocatalytic reduction of CO<sub>2</sub>, due to the competition at the electrode surface between CO<sub>2</sub> consumption (related to the rate-determinant step of the catalytic cycle) and the arrival of new substrate by diffusion.<sup>1c</sup>

**Table 1** Electrochemical data obtained by cyclic voltammetry in this study, in MeCN and Bu<sub>4</sub>PF<sub>6</sub> supporting electrolyte, and referenced to the redox system ferrocenium/ferrocene.<sup>a</sup>

Compl	Observed $E_{pc}$ values <sup>b</sup> (Cathodic scan)	$i_p(N_2)^c$ (at $E_{pc}$ )	$i_{cat}(CO_2)^c$ (at $E_{pc}$ )	Ratio <sup>d</sup> $\frac{i_{cat}(CO_2)}{i_p(N_2)}$
<b>1a</b>	-2.26, -3.00 <sup>e</sup>	45.7 (-3.00)	79.4 (-3.10)	1.74
<b>1b</b>	-2.20, -2.95	34.3 (-2.95)	68.3 (-2.83)	1.99
<b>2a</b>	-2.11, -2.42, -3.0	27.7 (-3.00)	51.3 (-3.10)	1.85
<b>2b</b>	-1.93, -2.60, -3.03	27.1 (-3.03)	73.5 (-2.88)	2.71
<b>3a</b>	-2.10, -2.41, -2.93 <sup>e</sup>	38.1 (-2.93)	65.0 (-3.10)	1.71
<b>3b</b>	-1.93, -2.30, -2.80	53.1 (-2.80)	195 (-2.88)	3.67

<sup>a</sup> The reduction potential mean value observed for Ferrocenium/Ferrocene (Fc<sup>+</sup>/Fc) used as internal calibrant under the employed experimental conditions was  $E^0 = 0.443 \pm 0.005$  V vs. the AgCl/Ag (3M NaCl) electrode.

<sup>b</sup> Cathodic scan peaks observed under N<sub>2</sub> unless stated otherwise.

<sup>c</sup> Maximum registered cathodic current ( $\mu$ A) under N<sub>2</sub>,  $i_p(N_2)$ , or under CO<sub>2</sub>,  $i_{cat}(CO_2)$  taken from peak showing greatest enhancement with CO<sub>2</sub> addition.

<sup>d</sup> Ratio between the Faradaic currents observed under N<sub>2</sub>,  $i_p(N_2)$ , or under CO<sub>2</sub>,  $i_{cat}(CO_2)$ .

<sup>e</sup> Waves where both peaks  $i_{ox}$  and  $i_{red}$  were observed. Value of  $E_{1/2}$  is given in those cases.

The catalytic activity of the complexes is supported by the decrease of the catalytic activity when the concentration of CO<sub>2</sub> is progressively substituted by bubbling Ar (Fig. S13, ESI) and by the dependence of the electrocatalytic reduction of CO<sub>2</sub> on the scan rate (Figs. S2, 3, 4, ESI) and on the concentration (Fig. S14, ESI).

As indicated in the Introduction, there are not previous reports on the catalytic activity on CO<sub>2</sub> reduction for complexes structurally similar to those herein described. The closest analogues might be mono(bipy)Ru(II) complexes containing two carbonyls and two chlorido ligands, which have been used both as electro- and photocatalysts for CO<sub>2</sub> reduction.<sup>4,7</sup> The ratios  $i_{cat}(CO_2)/i_p(N_2)$  obtained for compounds **2** and **3** (between 1.71 and 3.67, see Table 1) are slightly below those obtained in our group for *cis*-Ru(bipy)<sub>2</sub> complexes and for *fac*-Re(CO)<sub>3</sub> complexes (between 2.1 and 10.8 and between 2.7 and 11.5, respectively).<sup>22,23</sup> Although the reaction mechanism is still being

discussed after more than 20 years since the first studies, there is a general consensus about the formation of reduced species which would be highly active for the reduction of CO<sub>2</sub>. These reduced species may contain Ru<sup>I</sup>–Ru<sup>I</sup> or Ru<sup>0</sup>–Ru<sup>0</sup> bonds for the less hindered diimine ligands, or Ru–H bonds for those containing sterically demanding substituents.<sup>4,7</sup> In our case, all the attempts to reduce chemically either 1,2-azole (**1**) or 1,2-azolylamidino (**2**, **3**) complexes led to decomposition. The possibility of Ru(0) nano-particles as being the active catalysts was tested in a separate experiment and it is discussed below.

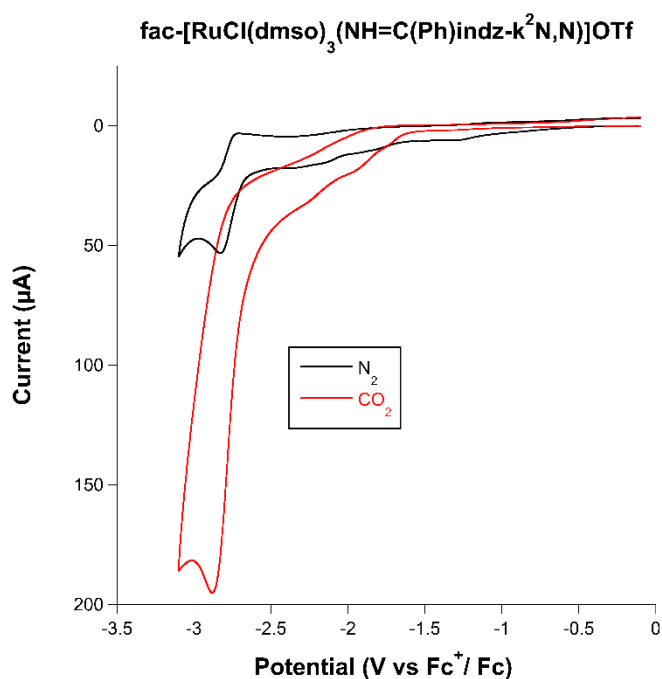


**Figure 2** Cyclic voltammograms of 0.5mM *fac*-[RuCl(dmsO)<sub>3</sub>(NH=C(Ph)indz-*k*<sup>2</sup>N,N)](OTf) (**3b**) (glassy carbon working electrode dish 3.0 mm diameter, dry MeCN, 0.1 M Bu<sub>4</sub>NPF<sub>6</sub>,) in Ar (blue) and after bubbling CO<sub>2</sub> (red).

In order to further evaluate the electrocatalytic activity, we performed a sequence of experiments on the indz complexes (**1b**, **2b**, and **3b**). We focused our study on these complexes since they exhibit higher  $i_{cat}(CO_2)/i_p(N_2)$  ratios, as well as less negative potentials for the first reduction by ca. 0.2 V, which we can attribute to the lower energy  $\pi$  system on the indz fragment. Firstly, scan rate experiments were performed on each reduction step, in order to determine their redox behaviour (Figs. S2, S3, S4, ESI). These studies showed the general instability of these complexes under catalytic conditions. Additional experiments were run either in DMSO (Table S1, ESI) as solvent instead of MeCN, either in MeCN saturated with Cl<sup>-</sup> (TBACl, Fig. S6, ESI). In all cases, the CVs point to the formation of species that show nonlinear response to the scan rate experiments, showing the generation of non-freely diffusing redox species, which lead to the complexity seen in the CVs. All systems displayed no reversibility, likely due to the instability of the species formed.

Controlled potential electrolysis (CPE) studies on indz complexes **1b**, **2b** and **3b**, were also performed following a

procedure previously described.<sup>22</sup> The experiments, carried out in MeCN using a three-electrode setup with a glassy carbon working electrode, were run at a potential 0.2 V lower than the electron addition, showing the greatest enhancement with the addition of CO<sub>2</sub>, as previously determined by CV for each indz complex. Each experiment was carried out during 6 h, while the MeCN solutions were maintained under CO<sub>2</sub> atmosphere and stirred. Samples of the solutions were pulled and tested with CV at 0 h, 2 h, 4 h, and 6 h (Figs. S7, S8, S9, ESI), under CO<sub>2</sub> atmosphere, then bubbled with N<sub>2</sub> for 15 min, and the scans were then repeated. The voltammograms indicate that the electrochemical activity is not lost as the reaction progresses. However, an increase in current is detected under N<sub>2</sub> atmosphere, indicating that a non-catalytical species that is accepting electrons is being formed (Figs. S7, S8, S9, ESI). After the 6h CPE experiment, Hg was added to the reaction mixture, which was then stirred for 12 h more at r.t. Hg is known to bind to Ru nanoparticles from the solutions, removing them as active species.<sup>24</sup> No observable changes to the behaviour of the complexes activity under CO<sub>2</sub> were detected after the addition of Hg, suggesting that the activity of the complexes is not due to the formation of nanoparticles. HPLC experiments were also performed before and after the experiment outlined above (Fig. S11, ESI) in order to further probe the solution stability of the indz family of complexes. The chromatograms taken at 254 nm indicate that the majority of each complex is degraded to different degradation products by the end of the experiment.

In order to test the hypothesis that the rapid formation of degradation products, including Ru(0) nanoparticles, could have been formed on the electrodes surface, CPE experiments were run for 2 h, at which time CV experiments were performed, first with the electrode “as is”, and then after cleaning the electrode with a low lint delicate task wipe saturated with dry MeCN (Fig. S10, ESI). These experiments clearly show that a catalytically-active film forms on the surface of the electrode, likely containing Ru(0) nanoparticles and possibly other Ru degradation products. This might be the cause of the less efficient catalytic abilities detected in the bulk solutions test discussed above, since rapid decomposition of the Ru complexes at the surface of the CPE electrode could be the cause behind their lack of activity. This degradation process was also examined by sonicating with EtOH the working electrode immediately after the 2 h CPE experiment, in order to remove any solid species deposited on it. This EtOH mixtures were then drop-casted for TEM samples. The TEM images show a variety of electron rich disordered clusters, thus supporting the hypothesis that Ru(0) particles are deposited on the electrode (Fig. S12, ESI).

#### Photocatalytic activity

Given the electrochemical instability of the complexes, we turned our attention to the photocatalytic activity of these complexes. Although some complexes can act as photocatalysts and photosensitizers, this is not the case for **1b**, **2b** and **3b**. Most Ru-based photocatalysts require the assistance of



photosensitizers since their direct excitation leads to ligand dissociation.<sup>25</sup> Shown in Fig. 3 are the results of the photocatalytic CO<sub>2</sub> reduction experiments by compounds **1b**, **2b** and **3b** carried out in a CO<sub>2</sub>-saturated acetonitrile/triethanolamine (MeCN/TEOA, 4:1 v/v) solution containing a mixture of the catalyst and [Ru(bipy)<sub>3</sub>]<sup>2+</sup> as the photosensitizer in a glass vial with a volume of 10 mL under continuous irradiation (light intensity of 150 mW/cm<sup>2</sup> at 25 °C, λ > 300 nm). To validate the photocatalytic data, various control experiments were carried out under different experimental conditions under irradiation with light. In the absence of [Ru(bipy)<sub>3</sub>]<sup>2+</sup>, the catalyst, or the sacrificial electron donor, TEOA, only a trace amount or no amount of product was produced, indicating that all the three components are necessary for efficient CO<sub>2</sub> activation. The formic acid produced was quantified using the protocol reported by Kubiak *et al.*<sup>26</sup> The results show that compounds **1b**, **2b** and **3b** are efficient CO<sub>2</sub> reduction catalysts under the conditions used (Table S1, ESI), although they also produce larger quantities of dihydrogen and trace amounts of formate.<sup>5d</sup> The source of protons is probably the TEOA. The turnover numbers for the production of CO is ~100 after 8 h and follows the order **1b** > **2b** ≈ **3b**. Other complexes of the type *trans*(Cl)-[Ru(bipy\*)(CO)<sub>2</sub>Cl<sub>2</sub>] (where bipy\* is a substituted bipy) have shown TON from *ca.* 100 to *ca.* 3000.<sup>7</sup>

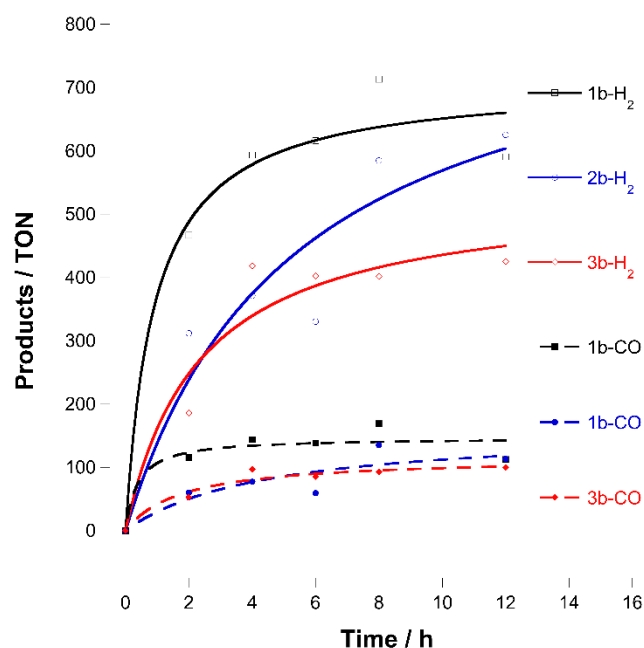


**Figure 3** Turnover number CO and H<sub>2</sub> evolved from 0.1 mM Ru complexes, 1.6 mM [Ru(bipy)<sub>3</sub>]<sup>2+</sup> in a CO<sub>2</sub>-saturated MeCN-TEOA solution (4:1 v/v) irradiated by >300 nm visible light.

Due to the higher photochemical activity of these complexes, a series of additional experiments were conducted, trying to establish the stability of the catalysts and to further understand the process. Firstly, the possibility of the presence of Ru(0) nano-particles as the active catalysts in the solution

was tested by adding 3 equivalents of Hg to the reaction solutions, and checking for changes in the products formation. These experiments (Figs. S7, S8, S9, ESI) did not show significant differences with respect to those obtained with Hg free solutions. This result leads to the conclusion that Ru(0) nano-particles are not an active catalyst in this system.

The photochemical activity of **1b** was also used to probe the carbon source of the complexes by analyzing the product formation of the CO<sub>2</sub> catalysis, by running the photocatalysis with a solution saturated with <sup>13</sup>CO<sub>2</sub>, and analyzing the products by gas chromatography (GC), as well as by mass spectrometry coupled GC (Tables S4, S5, ESI). All the carbon monoxide detected was in the form of <sup>13</sup>CO, showing that the degradation of the complexes is not a product source, in fact, the source of CO for this reaction is the catalysis of CO<sub>2</sub> to CO by the complexes.

## Conclusions

Base-catalyzed coupling of a nitrile and a 1,2-azole previously coordinated to Ru(II) dmsO complexes allow to synthesize new 1,2-azolylamidino complexes *fac*-[RuCl(dmsO)<sub>3</sub>(NH=C(R)az\*<sup>-</sup>κ<sup>2</sup>N,N)]OTf (R = Me, Ph; az\* = pz, indz) after chloride abstraction. The 1,2-azolylamidino complexes, as well as the parent 1,2-azole complexes are active both as the electro- and photocatalysts for the reduction of CO<sub>2</sub>, as demonstrated by proof-of-concept trials that led to the production of CO and trace amounts of formate. These results open the door to new complexes displaying this interesting behaviour, since so far the use of Ru(II) mono(bipy) complexes was limited to carbonyl complexes of the type [Ru(bipy)(CO)<sub>2</sub>X<sub>2</sub>]. The fact that 1,2-azolylamidino ligands with different electronic and steric features may be easily obtained in situ may encourage future developments in this area, given the decisive role of the presence of substituents of the diimine ligand on the electrocatalyzed reduction of CO<sub>2</sub>.

## Experimental Section

### General remarks

All manipulations were performed under a N<sub>2</sub> atmosphere following conventional Schlenk techniques. Solvents were purified according to standard procedures. *cis*-[Ru(dmsO)<sub>4</sub>Cl<sub>2</sub>]<sub>2</sub><sup>27</sup> was obtained as previously described. All other reagents were obtained from the usual commercial suppliers and used as received. Infrared spectra were recorded in solid in a Bruker Tensor 27 FTIR. Standard abbreviations are used to indicate intensity: vw = very weak, w = weak, m = medium, s = strong, vf = very strong. NMR spectra were recorded on 500 MHz Agilent DD2 and 400 MHz Agilent MR instruments in the Laboratory of Instrumental Techniques (LTI) Research Facilities, University of Valladolid, using CDCl<sub>3</sub> or (CD<sub>3</sub>)<sub>2</sub>CO as solvents at room temperature (r.t.). <sup>1</sup>H and <sup>13</sup>C NMR chemical shifts (δ) are reported in parts per million (ppm) and are referenced to tetramethylsilane (TMS), using the residual solvent peak as an internal reference. Coupling constants (J) are reported in Hz.

Standard abbreviations are used to indicate multiplicity: s = singlet, d = doublet, ddd = doublet of doublet of doublets, dt = doublet of triplets, t = triplet, m = multiplet. The full assignment of the  $^1\text{H}$  NMR spectra was supported by typical homonuclear  $^1\text{H}$ - $^1\text{H}$  correlations such as COSY, TOCSY and NOESY experiments and the assignment of  $^{13}\text{C}\{^1\text{H}\}$  data was supported by HMBC and HSQC heteronuclear experiments. Elemental analyses were performed on a Thermo Fisher Scientific EA Flash 2000.

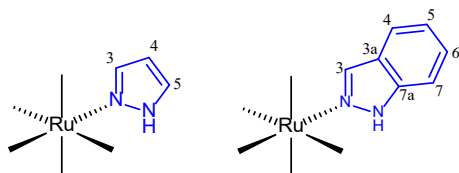


Figure 4 Numbering of pyrazole and indazole ligands for NMR assignment.

***cis,fac*-[RuCl<sub>2</sub>(dmsO)<sub>3</sub>(pzH)], 1a.** This complex was prepared by a modification of the method previously described in the literature. Some spectroscopic data were also previously reported.<sup>15</sup> A mixture of *cis*-[RuCl<sub>2</sub>(dmsO)<sub>4</sub>] (0.097 g, 0.2 mmol) and pzH (0.014 g, 0.2 mmol) in MeOH (10 mL) was stirred at r.t. for 3 h. The clear yellow solution was left to stand at  $-20^\circ\text{C}$ , giving a yellow microcrystalline solid, which was decanted, washed with Et<sub>2</sub>O (2 x 5 mL approximately), and dried in vacuo, yielding 0.070 g, 74%.  $^1\text{H}$  NMR (500 MHz, (CD<sub>3</sub>)<sub>2</sub>CO, r.t.)  $\delta$ : 3.17 (s, 2H<sub>CH<sub>3</sub></sub> dmsO, 6 H), 3.46 (s, 2H<sub>CH<sub>3</sub></sub> dmsO, 6 H), 3.52 (s, 2H<sub>CH<sub>3</sub></sub> dmsO, 6 H), 6.42 (t,  $J$  = 2.3 Hz, H<sup>4</sup>, 1 H), 7.68 (d,  $J$  = 2.3 Hz, H<sup>3</sup>, 1 H), 8.55 (d,  $J$  = 2.3 Hz, H<sup>5</sup>, 1 H), 13.98 (s, NH, 1 H).  $^{13}\text{C}\{^1\text{H}\}$  NMR (126 MHz, (CD<sub>3</sub>)<sub>2</sub>CO, r.t.)  $\delta$ : 45.6 (2C, 2C<sub>CH<sub>3</sub></sub> dmsO), 46.8 (2C, 2C<sub>CH<sub>3</sub></sub> dmsO), 47.4 (2C, 2C<sub>CH<sub>3</sub></sub> dmsO), 107.0 (C<sup>4</sup>), 130.5 (C<sup>3</sup>), 141.9 (C<sup>5</sup>). IR (cm<sup>-1</sup>): 615 w, 675 m, 708 w, 719 w, 771 m, 816 d, 880 vw, 935 m, 951 m, 968 m, 981 m, 1011 vs, 1036 m, 1060 m, 1091 s, 1171 vw, 1359 w, 1408 m, 2838 w, 2918 w, 3122 w. Calcd for C<sub>9</sub>Cl<sub>2</sub>H<sub>22</sub>N<sub>2</sub>O<sub>3</sub>RuS<sub>3</sub>: C, 22.84; H, 4.65; N, 5.92; S, 20.30. Found: C, 22.88; H, 4.62; N, 5.77; S, 20.54.

***cis,fac*-[RuCl<sub>2</sub>(dmsO)<sub>3</sub>(indzH)], 1b.** This complex was prepared by a modification of the method previously described in the literature. Some spectroscopic data were also previously reported.<sup>16</sup> A mixture of *cis*-[RuCl<sub>2</sub>(dmsO)<sub>4</sub>] (0.097 g, 0.2 mmol) and indzH (0.024 g, 0.2 mmol) in MeOH (10 mL) was stirred at r.t. for 1 h. The clear yellow solution was left to stand at  $-20^\circ\text{C}$ , giving a yellow microcrystalline solid, which was decanted, washed with Et<sub>2</sub>O (2 x 5 mL approximately), and dried in vacuo, yielding 0.078 g, 74%.  $^1\text{H}$  NMR (500 MHz, (CD<sub>3</sub>)<sub>2</sub>CO, r.t.)  $\delta$ : 3.51 (s, 2H<sub>CH<sub>3</sub></sub> dmsO, 6 H), 3.50 (s, 2H<sub>CH<sub>3</sub></sub> dmsO, 6 H), 3.21 (s, 2H<sub>CH<sub>3</sub></sub> dmsO, 6 H), 7.22 (ddd,  $J$  = 8.2, 6.9, 0.9 Hz, H<sup>5</sup>, 1 H), 7.47 (ddd,  $J$  = 8.1, 6.9, 1.1 Hz, H<sup>6</sup>, 1 H), 7.73 (dd,  $J$  = 8.1, 0.9 Hz, H<sup>7</sup>, 1 H), 7.85 (dd,  $J$  = 8.2, 1.1 Hz, H<sup>4</sup>, 1 H), 9.16 – 9.10 (m, H<sup>3</sup>, 1 H), 14.12 (s, NH, 1 H).  $^{13}\text{C}\{^1\text{H}\}$  NMR (126 MHz, (CD<sub>3</sub>)<sub>2</sub>CO, r.t.)  $\delta$ : 44.9 (2C, 2C<sub>CH<sub>3</sub></sub> dmsO), 46.1 (2C, 2C<sub>CH<sub>3</sub></sub> dmsO), 46.5 (2C, 2C<sub>CH<sub>3</sub></sub> dmsO), 110.4 (C<sup>7</sup>), 120.8 (C<sup>4</sup>), 121.5 (C<sup>5</sup>), 127.9 (C<sup>6</sup>), 128.2 (C<sup>7a</sup>), 138.4 (C<sup>3</sup>), 140.4 (C<sup>3a</sup>). IR (cm<sup>-1</sup>): 3929 mw, 3238 w, 3133 w, 3028 w, 3013 w, 2922 w, 2324 w, 2286 w, 2164 w, 2149 w, 2113 w, 2051 w, 1981 w, 1933 w, 1797 w, 1700 w, 1626 m, 1585 w, 1509 m, 1483 w, 1446 m, 1412 m, 1380 m, 1359 m, 1307 m, 1287 m, 1270 m, 1253 w, 1218 w, 1193 m, 1148 w, 1084 vs, 1059 s, 1011

s, 973 m, 952 s, 920 m, 902 m, 863 w, 852 w, 781 w, 757 m, 749 m, 720 m, 678 m, 620 w. Calcd for C<sub>13</sub>Cl<sub>2</sub>H<sub>24</sub>N<sub>2</sub>O<sub>3</sub>RuS<sub>3</sub>: C, 29.83; H, 4.59; N, 5.35; S, 18.36. Found: C, 29.75; H, 4.61; N, 5.19; S, 18.43.

***fac*-[RuCl(dmsO)<sub>3</sub>(NH=C(Me)pz- $\kappa^2$ N,N)](OTf), 2a.** AgOTf (0.051 g, 0.20 mmol) was added to a solution of **1a** (0.095 g, 0.20 mmol) in MeCN (10 mL). 100  $\mu\text{L}$  of aqueous 0.02M NaOH (0.002 mmol) were then added and the mixture was stirred at r.t. for 12 h in the absence of light. The reaction mixture was filtered to remove solid AgCl and dried in vacuo. The solid was crystallized in MeCN/Et<sub>2</sub>O at  $-20^\circ\text{C}$ , giving a colorless microcrystalline solid, which was decanted, washed with Et<sub>2</sub>O (2 x 5 mL approximately), and dried in vacuo, yielding 0.079 g, 63%.  $^1\text{H}$  NMR (500 MHz, (CD<sub>3</sub>)<sub>2</sub>CO, r.t.)  $\delta$ : 2.83 (s, H<sub>CH<sub>3</sub></sub> dmsO, 3 H), 3.02 (s, N=C(CH<sub>3</sub>), 3 H), 3.19 (s, H<sub>CH<sub>3</sub></sub> dmsO, 3 H), 3.39 (s, H<sub>CH<sub>3</sub></sub> dmsO, 3 H), 3.55 (s, H<sub>CH<sub>3</sub></sub> dmsO, 3 H), 3.57 (s, H<sub>CH<sub>3</sub></sub> dmsO, 3 H), 3.61 (s, H<sub>CH<sub>3</sub></sub> dmsO, 3 H), 6.94 (t,  $J$  = 2.5 Hz, H<sup>4</sup>, 1 H), 8.78 (d,  $J$  = 2.5 Hz, H<sup>3</sup>, 1 H), 8.87 (d,  $J$  = 2.5 Hz, H<sup>5</sup>, 1 H), 11.00 (s, NH, 1 H).  $^{13}\text{C}\{^1\text{H}\}$  NMR (126 MHz, (CD<sub>3</sub>)<sub>2</sub>CO, r.t.)  $\delta$ : 17.8 (N=C(CH<sub>3</sub>)), 44.6 (C<sub>CH<sub>3</sub></sub> dmsO), 45.2 (C<sub>CH<sub>3</sub></sub> dmsO), 45.7 (C<sub>CH<sub>3</sub></sub> dmsO), 46.2 (C<sub>CH<sub>3</sub></sub> dmsO), 47.0 (C<sub>CH<sub>3</sub></sub> dmsO), 47.1 (C<sub>CH<sub>3</sub></sub> dmsO), 111.0 (C<sup>4</sup>), 134.9 (C<sup>3</sup>), 148.7 (C<sup>5</sup>), 164.3 (N=C(CH<sub>3</sub>)). IR (cm<sup>-1</sup>): 633 s, 685 m, 724 w, 759 w, 779 m, 920 w, 939 m, 964 m, 977 m, 1021 vs, 1052 w, 1086 vs, 1107 s, 1107 m, 1152 m, 1173 m, 1229 s, 1244 m, 1279 w, 1411 w, 1656 m, 2923 w, 3005 w, 3102 w, 3205 w. Calcd for C<sub>12</sub>ClF<sub>3</sub>H<sub>25</sub>N<sub>3</sub>O<sub>6</sub>RuS<sub>4</sub>: C, 22.95; H, 3.98; N, 6.69; S, 20.40. Found: C, 22.75; H, 3.91; N, 6.72; S, 20.55.

***fac*-[RuCl(dmsO)<sub>3</sub>(NH=C(Me)indz- $\kappa^2$ N,N)](OTf), 2b.** AgOTf (0.049 g, 0.19 mmol) was added to a solution of **1b** (0.100 g, 0.19 mmol) in MeCN (10 mL) and the mixture was stirred at r.t. or 12 h in the absence of light. The reaction mixture was filtered to remove solid AgCl and dried in vacuo. The solid was crystallized in MeCN/Et<sub>2</sub>O at  $-20^\circ\text{C}$ , giving a colorless microcrystalline solid, which was decanted, washed with Et<sub>2</sub>O (2 x 5 mL approximately), and dried in vacuo, yielding 0.801 g, 62%.  $^1\text{H}$  NMR (500 MHz, (CD<sub>3</sub>)<sub>2</sub>CO, r.t.)  $\delta$ : 3.10 (s, H<sub>CH<sub>3</sub></sub> dmsO, 3 H), 3.24 (s, H<sub>CH<sub>3</sub></sub> dmsO, 3 H), 3.33 (s, N=C(CH<sub>3</sub>), 3 H), 3.44 (s, H<sub>CH<sub>3</sub></sub> dmsO, 3 H), 3.60 (s, 2 H<sub>CH<sub>3</sub></sub> dmsO, 6 H), 3.65 (s, H<sub>CH<sub>3</sub></sub> dmsO, 3 H), 7.61 (t,  $J$  = 8.0 Hz, H<sup>6</sup>, 1 H), 7.83 (t,  $J$  = 8.0 Hz, H<sup>5</sup>, 1 H), 8.17 (d,  $J$  = 8.2 Hz, H<sup>4</sup>, 1 H), 8.19 (d,  $J$  = 8.2, H<sup>7</sup>, 1 H), 9.69 (s, H<sup>3</sup>, 1 H), 10.51 (s, NH, 1 H).  $^{13}\text{C}\{^1\text{H}\}$  NMR (126 MHz, (CD<sub>3</sub>)<sub>2</sub>CO, r.t.)  $\delta$ : 20.5 (N=C(CH<sub>3</sub>)), 45.0–50.0 (6 C, C<sub>CH<sub>3</sub></sub> dmsO), 112.9 (C<sup>4</sup>), 123.3 (C<sup>7</sup>), 125.3 (C<sup>6</sup>), 125.6 (C<sup>7a</sup>), 131.3 (C<sup>5</sup>), 140 (C<sup>3a</sup>), 146.3 (C<sup>3</sup>), 165.0 (N=C(CH<sub>3</sub>)). IR (cm<sup>-1</sup>): 3221 w, 3117 vw, 3022 w, 2971 vw, 1690 w, 1632 m, 1584 vw, 1511 w, 1484 m, 1468 w, 1428 m, 1409 w, 1356 w, 1316 w, 1276 s, 1249 vs, 1226 m, 1196 m, 1175 m, 1156 s, 1112 s, 1100 s, 1081 s, 1029 vs, 1019 vs, 977 m, 966 m, 943 w, 914 m, 864 w, 795 w, 756 s, 719 w, 683 m, 634 vs. Calcd for C<sub>16</sub>ClF<sub>3</sub>H<sub>27</sub>N<sub>3</sub>O<sub>6</sub>RuS<sub>4</sub>: C, 28.34; H, 3.99; N, 6.20; S, 18.89. Found: C, 28.45; H, 4.00; N, 6.39; S, 18.68.

***fac*-[RuCl(dmsO)<sub>3</sub>(NH=C(Ph)pz- $\kappa^2$ N,N)](OTf), 3a.** AgOTf (0.051 g, 0.2 mmol) was added to a solution of **1a** (0.095 g, 0.2 mmol) in (CH<sub>3</sub>)<sub>2</sub>CO (10 mL). 100  $\mu\text{L}$  of PhCN and 100  $\mu\text{L}$  of aqueous 0.02M NaOH (0.002 mmol) was then added and the mixture was stirred at r.t. for 24 h in the absence of light. The reaction mixture was filtered to remove solid AgCl and dried in vacuo. The solid was crystallized in (CH<sub>3</sub>)<sub>2</sub>CO/Et<sub>2</sub>O at  $-20^\circ\text{C}$ ,

giving a yellow microcrystalline solid, which was decanted, washed with Et<sub>2</sub>O (2 x 5 mL approximately), and dried in vacuo, yielding 0,084 g, 61%. <sup>1</sup>H NMR (500 MHz, (CD<sub>3</sub>)<sub>2</sub>CO, r.t.) δ: 3.31 (s, H<sub>CH<sub>3</sub></sub> dmsO, 3 H), 3.34 (s, H<sub>CH<sub>3</sub></sub> dmsO, 3 H), 3.47 (s, H<sub>CH<sub>3</sub></sub> dmsO, 3 H), 3.63 (s, H<sub>CH<sub>3</sub></sub> dmsO, 3 H), 3.64 (s, H<sub>CH<sub>3</sub></sub> dmsO, 3 H), 3.69 (s, H<sub>CH<sub>3</sub></sub> dmsO, 3 H), 6.97 (dd, *J* = 3.2, 2.1 Hz, H<sup>4</sup> pz, 1 H), 7.59 – 8.04 (m, C<sub>6</sub>H<sub>5</sub> Ph, 5 H), 8.45 (dd, *J* = 3.2, 0.6 Hz, H<sup>3</sup> pz, 1 H), 9.03 (dd, *J* = 2.1, 0.6 Hz, H<sup>5</sup> pz, 1 H), 11.21 (s, NH, 1 H). <sup>13</sup>C{<sup>1</sup>H} NMR (126 MHz, (CD<sub>3</sub>)<sub>2</sub>CO, r.t.) δ: 44.6 (C<sub>CH<sub>3</sub></sub> dmsO), 45.2 (C<sub>CH<sub>3</sub></sub> dmsO), 45.7 (C<sub>CH<sub>3</sub></sub> dmsO), 46.2 (C<sub>CH<sub>3</sub></sub> dmsO), 47.0 (C<sub>CH<sub>3</sub></sub> dmsO), 47.1 (C<sub>CH<sub>3</sub></sub> dmsO), 111.6 (C<sup>4</sup>), 129.4–133.4 (5C, C Ph), 136.4 (C<sup>3</sup>), 149.7 (C<sup>5</sup>), 165.0 (N=C(Ph)), 166.0 (C<sub>ipso</sub> Ph). IR (cm<sup>-1</sup>): 3508 w, 3220 w, 3138 w, 3025 w, 2925 w, 2323 w, 2287 w, 2231 w, 2188 w, 2164 w, 2140 w, 2113 w, 2083 w, 2050 w, 1982 w, 1917 w, 1626 m, 1577 w, 1527 w, 1497 w, 1456 w, 1442 m, 1415 m, 1321 w, 1274 s, 1246 vs, 1224 s, 1156 s, 1079 s, 1027 vs, 973 m, 922 m, 896 m, 760 m, 724 w, 704 m, 684 m, 636 s. Calcd for C<sub>17</sub>ClF<sub>3</sub>H<sub>27</sub>N<sub>3</sub>O<sub>6</sub>RuS<sub>4</sub>: C, 29.54; H, 3.94; N, 6.08; S, 18.56. Found: C, 33.92; H, 4.40; N, 5.44; S, 17.02. Found: C, 29.62; H, 3.78; N, 6.01; S, 18.47.

**fac-[RuCl(dmsO)<sub>3</sub>(NH=C(Ph)indz-κ<sup>2</sup>N,N)](OTf), 3b**, AgOTf (0.051 g, 0.2 mmol) was added to a solution of **1b** (0.105 g, 0.2 mmol) in (CH<sub>3</sub>)<sub>2</sub>CO (10 mL). 100 μL of PhCN was then added and the mixture was stirred at r.t. for 24 h in the absence of light. The reaction mixture was filtered to remove solid AgCl and dried in vacuo. The solid was crystallized in (CH<sub>3</sub>)<sub>2</sub>CO/Et<sub>2</sub>O at –20 °C, giving a yellow microcrystalline solid, which was decanted, washed with Et<sub>2</sub>O (2 x 5 mL approximately), and dried in vacuo, yielding 0,093 g, 63%. <sup>1</sup>H NMR (500 MHz, (CD<sub>3</sub>)<sub>2</sub>CO, r.t.) δ: 3.31 (s, H<sub>CH<sub>3</sub></sub> dmsO, 3 H), 3.34 (s, H<sub>CH<sub>3</sub></sub> dmsO, 3 H), 3.47 (s, H<sub>CH<sub>3</sub></sub> dmsO, 3 H), 3.63 (s, H<sub>CH<sub>3</sub></sub> dmsO, 3 H), 3.64 (s, H<sub>CH<sub>3</sub></sub> dmsO, 3 H), 3.69 (s, H<sub>CH<sub>3</sub></sub> dmsO, 3 H), 6.38 (dt, *J* = 8.5, 0.8 Hz, H<sup>6</sup> indz, 1 H), 7.46 – 7.94 (m, H<sup>4</sup> indz, H<sup>5</sup> indz, C<sub>6</sub>H<sub>5</sub> Ph, 7 H), 8.17 (dd, *J* = 8.5, 0.8 Hz, H<sup>7</sup> indz, 1 H), 9.80 (d, *J* = 0.8 Hz, H<sup>3</sup> indz, 1 H), 10.85 (s, NH, 1 H). <sup>13</sup>C{<sup>1</sup>H} NMR (126 MHz, (CD<sub>3</sub>)<sub>2</sub>CO, r.t.) δ: 44.5 (C<sub>CH<sub>3</sub></sub> dmsO), 45.2 (C<sub>CH<sub>3</sub></sub> dmsO), 45.8 (C<sub>CH<sub>3</sub></sub> dmsO), 46.3 (C<sub>CH<sub>3</sub></sub> dmsO), 47.0 (C<sub>CH<sub>3</sub></sub> dmsO), 47.4 (C<sub>CH<sub>3</sub></sub> dmsO), 112.2 (C<sup>6</sup> indz), 122.7 (C<sup>7a</sup>), 123.2 (C<sup>7</sup> indz), 125.5–133.2 (7C, C<sup>4,5</sup> indz, C Ph), 140.7 (C<sup>3a</sup>), 147.7 (C<sup>3</sup> indz), 165.0 (N=C(Ph)), 166.0 (C<sub>ipso</sub> Ph). IR (cm<sup>-1</sup>): 3264 vw, 3080 vw, 3016 vw, 2964 vw, 1310 vw, 1288 vw, 1119 m, 1094 m, 1018 m, 974 m, 918 m, 713 vw, 677 w. Calcd for C<sub>21</sub>ClF<sub>3</sub>H<sub>29</sub>N<sub>3</sub>O<sub>6</sub>RuS<sub>4</sub>: C, 34.03; H, 3.94; N, 5.68; S, 17.31. Found: C, 33.92; H, 3.75; N, 5.44; S, 17.02.

### Electrochemical experiments

Electrochemical experiments were performed by using a Model 6012D or 604E Electrochemical analyzer from CH Instruments, Inc. Cyclic voltammetry experiments were performed under either N<sub>2</sub>(g) or Ar(g) and CO<sub>2</sub>(g) in a one-compartment cell with a glassy carbon working electrode, a platinum wire counter electrode and a Ag/Ag<sup>+</sup> (10 mM AgNO<sub>3</sub> in acetonitrile, DMF or DMSO) reference electrode with ferrocene as an external reference. The glassy carbon working electrode was polished with 1.0 micron alumina powder, extensively rinsed with deionized water, then polished for 60 seconds with 0.05 micron alumina powder (CH Instruments). The electrode was again

rinsed with dry MeCN/DMF prior to all electrochemistry experiments. All experiments were performed by using 0.1 M TBAPF<sub>6</sub> as the supporting electrolyte unless otherwise specified, acetonitrile as the solvent, and with Ru complexes concentration of 1.0 mM unless indicated otherwise.

The solubility of saturated CO<sub>2</sub> in acetonitrile has been reported to be 0.28M at 25 °C.<sup>28</sup> Changing atmosphere from pure N<sub>2</sub> (or Ar) to pure CO<sub>2</sub> or *vice versa* required bubbling with the new gas for not less than five minutes. Lasting such time, the CV's obtained were the same than those obtained in the first scan under a specific atmosphere. Bubbling was kept during the interim between scans. During scan time the PTFE was risen and kept above the surface of the solution to avoid agitation.

### Controlled Potential Electrolysis

Controlled potential electrolysis (CPE) experiments were performed by using a Model 6012D Electrochemical analyzer from CH Instruments, Inc. with 25 mL of an MeCN/TBAPF<sub>6</sub> solution in a cell with a carbon-rod working electrode (~1.9 cm<sup>2</sup> submersed area), a silver-wire pseudoreference, and a platinum-wire counter electrode separated from the solution by a medium-porosity frit. Gas chromatography analysis of the headspace was performed on an Agilent 7820 instrument equipped with a HP-Molesieve column and a gas sampling valve, as well as a thermal conductivity detector (TCD), stainless-steel column packed with molecular sieves (60/80 mesh), and UHP He as the carrier gas (flow rate = 35 mL min<sup>-1</sup>). The operating temperatures of the injection port, the oven/column, and detector were 100 °C, 80 °C, and 100 °C, respectively. Calibration curves for carbon monoxide and hydrogen were created by injecting known quantities of CO or H<sub>2</sub> into the electrochemical cell and then sampling the headspace.

### Photocatalysis Procedure

Photochemical reactions were performed in a 20 mL reaction vessel containing 10 mL of CO<sub>2</sub>-saturated MeCN-TEOA solution (4:1 v/v), the Ru catalyst was present in a concentration of 0.1 mM, whereas the initial concentration of the photosensitizer, [Ru(bipy)<sub>3</sub>]<sup>2+</sup>, was 1.6 mM. The solution was irradiated by >300 nm visible light. Analysis of the resulting compounds was performed as described in the CPE section.

### Crystal Structure Determination for Compounds 2a and 2b

Crystals were grown by slow diffusion of Et<sub>2</sub>O into concentrated solutions of the complexes in MeCN (for **2a** and **2b**) at –20 °C. Relevant crystallographic details can be found in the CIF. A crystal was attached to a glass fiber and transferred to an Agilent SuperNova diffractometer fitted with an Atlas CCD detector. The crystals were kept at 293(2) K during data collection. Using Olex2,<sup>29</sup> the structures were solved with the ShelXT<sup>30</sup> structure solution program and then the structures were refined with the ShelXL<sup>31</sup> refinement package using least squares minimization. All non-hydrogen atoms were refined anisotropically. Hydrogen atoms were set in calculated positions and refined as riding atoms, with a common thermal parameter. All graphics were made with Olex2, and distances

and angles of hydrogen bonds were calculated with PARST<sup>32</sup> (normalized values).<sup>33</sup>

## Conflicts of interest

There are no conflicts of interest to declare.

## Acknowledgements

The authors in Valladolid gratefully acknowledge financial support from the Spanish MINECO, Spain (PGC2018-099470-B-I00), the Junta de Castilla y León (VA130618), and the Spanish Ministerio de Ciencia e Innovación (MCIN, PID2021-124691NB-I00, funded by MCIN/AEI/10.13039/501100011033/FEDER, UE). E. C. thanks the UVa for her grant. G. G.-H. gratefully acknowledges financial support by the Junta de Castilla y León, and by the Spanish Ministerio de Ciencia e Innovación MICIN, and the European Union Next Generation EU/PRTR. A.M.A.-B. is grateful for support from the National Science Foundation CAREER grant (CHE-1652606).

## Notes and references

- (a) J. Qiao, Y. Liu, F. Hong and J. Zhang, *Chem. Soc. Rev.*, 2014, **43**, 631–675. (b) N. Elgrishi, M.B. Chambers, X. Wang and M. Fontecave, *Chem. Soc. Rev.*, 2017, **46**, 761–796. (c) R. Francke, B. Schille and M. Roemelt, *M. Chem. Rev.*, 2018, **118**, 4631–4701. (d) C. Jiang, A.W. Nichols and C.W.; Machan, *Dalton Trans.*, 2019, **48**, 9454–9468. (e) S. Zhang, Q. Fan, R. Xia and T.J. Meyer, *Acc. Chem. Res.*, 2020, **53**, 255–264. (f) Y.J. Sa, C.W. Lee, S.Y. Lee, J. Na, U. Lee and Y.J. Hwang, *Chem. Soc. Rev.*, 2020, **49**, 6632–6665. (g) F. Franco, C. Rettenmaier, H.S. Jeon and B.R. Cuenya, *Chem. Soc. Rev.*, 2020, **49**, 6884–6946. (h) R.-Z. Zhang, B.-Y. Wu, Q. Li, L.-L. Lu, W. Shi and P. Cheng, *Coord. Chem. Rev.*, 2020, **422**, 213436 (1–28). (i) N.W. Kinzel, C. Werl and W. Leitner, *Angew. Chem. Int. Ed.*, 2021, **60**, 11628–11686. (j) P. Saha, S. Amanullah and A. Dey, *Acc. Chem. Res.*, 2022, **55**, 134–144. (k) E. Fujita, D.C. Grills, G.F. Manbeck and D.E. Polyansky, *Acc. Chem. Res.*, 2022, **55**, 616–628. (l) G. Marcandalli, M.C.O. Monteiro, A. Goyal and M.T.M. Koper, *Acc. Chem. Res.*, 2022, **55**, 1900–1911. (m) H.-Q. Liang, T. Beweries, R. Francke and M. Beller, *Angew. Chem. Int. Ed.*, 2022, **61**, e202200723 (1–19). (n) X. She, Y. Wang, H. Xu, S.C.E. Tsang and S.P. Lau, *Angew. Chem. Int. Ed.*, 2022, **61**, 202211396 (1–29). (o) K. Lei and B. Yu, *Chem. Eur. J.*, 2022, **28**, e202200141 (1–15). (p) W. Nie and C.C.L. McCrory, *Dalton Trans.*, 2022, **51**, 6993–7010. (q) R. Ayyappan, I. Abdalghani, R.C. Da Costa and G.R. Owen, *Dalton Trans.*, 2022, **51**, 11582–11611. (r) Y. Yamazaki, M. Miyaji and O. Ishitani, *J. Am. Chem. Soc.*, 2022, **144**, 6640–6660.
- (a) H. Ishida, H. Tanaka, K. Tanaka and T. Tanaka, *Chem. Commun.*, 1987, 131–132. (b) H. Ishida, K. Tanaka and T. Tanaka, *Organometallics*, 1987, **6**, 181–186.
- (a) H. Ishida, K. Fujiki, T. Ohba, K. Ohkubo, K.; Tanaka, T. Terada and T. Tanaka, *J. Chem. Soc., Dalton Trans.*, 1990, **2**, 2155–2160. (b) J.R. Pugh, M.R.M. Bruce, B.P. Sullivan and T.J. Meyer, *Inorg. Chem.*, 1991, **30**, 86–91. (c) H. Nagao, T. Mizukawa and K. Tanaka, *Inorg. Chem.*, 1994, **33**, 3415–3420. (d) K. Toyohara, H. Nagao, T. Mizukawa and K. Tanaka, *Inorg. Chem.*, 1995, **34**, 5399–5400. (e) M.M. Ali, H. Sato, T. Mizukawa, K. Tsuge, M. Hagab and K. Tanaka, *Chem. Commun.*, 1998, 249–250. (f) K. Tanaka and D. Ooyama, *Coord. Chem. Rev.*, 2002, **226**, 211–218. (g) F.H. Haghghi, H. Hadadzadeh, H. Farrokhpour, N. Serri, K. Abdia and H.A. Rudbarib, *Dalton Trans.*, 2014, **43**, 11317–11332. (h) D.J. Boston, Y.M.F. Pachón, R.O. Lezna, N.R. de Tacconi and F.M. MacDonnell, *Inorg. Chem.*, 2014, **53**, 6544–6553. (i) B.A. Johnson, S. Maji, H. Agarwala, T.A. White, E. Mijangos and S. Ott, *Angew. Chem. Int. Ed.*, 2016, **55**, 1825–1829. (j) B.A. Johnson, H. Agarwala, T.A. White, E. Mijangos, S. Maji and S. Ott, *Chem. Eur. J.*, 2016, **22**, 14870–14880.
- (a) M.-N. Collomb-Dunand-Sauthier, A. Deronzier and R. Ziessel, *J. Chem. Soc., Chem. Commun.*, 1994, 189–191. (b) M.-N. Collomb-Dunand-Sauthier, A. Deronzier and R. Ziessel, *Inorg. Chem.*, 1994, **33**, 2961–2967. (c) S. Chardon-Noblat, M.-N. Collomb-Dunand-Sauthier, A. Deronzier, R. Ziessel and D. Zsoldos, *Inorg. Chem.*, 1994, **33**, 4410–4412. (d) S. Chardon-Noblat, A. Deronzier, R. Ziessel and D. Zsoldos, *Inorg. Chem.*, 1997, **36**, 5384–5389. (e) S. Chardon-Noblat, A. Deronzier, R. Ziessel and D. Zsoldos, *J. Electroanal. Chem.*, 1998, **444**, 253–260. (f) C.W. Machan, M.D. Sampson and C.P. Kubiak, *J. Am. Chem. Soc.*, 2015, **137**, 8564–8571.
- (a) A.J. Morris, G.J. Meyer and E. Fujita, *Acc. Chem. Res.*, 2009, **42**, 1983–1994. (b) H. Takeda and O. Ishitani, *Coord. Chem. Rev.*, 2010, **254**, 346–354. (c) Y. Yamazaki, H. Takeda and O. Ishitani, *J. Photochem. Photobiol. C Photochem. Rev.*, 2015, **25**, 106–137. (d) Y. Kuramochi, O. Ishitani and H. Ishida, *Coord. Chem. Rev.*, 2018, **373**, 333–356. (e) Y.-H. Luo, L.-Z. Dong, J. Liu, S.-L. Li and Y.-Q. Lan, *Coord. Chem. Rev.*, 2019, **390**, 86–126. (f) H. Kumagai, Y. Tamaki and O. Ishitani, *Acc. Chem. Res.*, 2022, **55**, 978–990. (g) N. Nandal and S.L. Jain, *Coord. Chem. Rev.*, 2022, **451**, 214271 (1–18).
- (a) H. Ishida, T. Terada, K. Tanaka and T. Tanaka, *Inorg. Chem.*, 1990, **29**, 905–911. (b) J.-M. Lehn and R. Ziessel, *J. Organometallic Chem.*, 1990, **382**, 157–173. (c) K. Kobayashi, T. Kikuchi, S. Kitagawa and K. Tanaka, *Angew. Chem. Int. Ed.*, 2014, **53**, 11813–11817. (d) Y. Kuramochi, M. Kamiya and H. Ishida, *Inorg. Chem.*, 2014, **53**, 3326–3332. (e) R.R. Rodrigues, C.M. Boudreaux, E.T. Papish and J.H. Delcamp, *ACS Appl. Energy Mater.*, 2019, **2**, 37–46. (f) R.N. Sampaio, D.C. Grills, D.E. Polyansky, D.J. Szaldaand E. Fujita, *J. Am. Chem. Soc.*, 2020, **142**, 2413–2428.
- (a) R. Kuriki, K. Sekizawa, O. Ishitani and K. Maeda, *Angew. Chem. Int. Ed.*, 2015, **54**, 2406–2409. (b) Y. Kuramochi, K. Fukaya, M. Yoshida and H. Ishida, *Chem. - A Eur. J.*, 2015, **21**, 10049–10060. (c) Y. Kuramochi, J. Itabashi, K. Fukaya, A. Enomoto, M. Yoshida and H. Ishida, *Chem. Sci.*, 2015, **6**, 3063–3074. (d) Y. Kuramochi, J. Itabashi, M. Toyama and H. Ishida, *ChemPhotoChem*, 2018, **2**, 314–322.
- (a) P.L. Cheung, S.C. Kapper, T. Zeng, M.E. Thompson and C.P. Kubiak, *J. Am. Chem. Soc.*, 2019, **141**, 14961–14965. (b) M.R. Madsen, J.B. Jakobsen, M.H. Rønne, H. Liang, H.C.D. Hammershøj, P. Nørby, S.U. Pedersen, T. Skrydstrup and K. Daasbjerg, *Organometallics*, 2020, **39**, 1480–1490. (c) C. Back, Y. Seo, S. Choi, M.S. Choe, D. Lee, J.-O. Baeg, H.-J. Son and S.O. Kang, *Inorg. Chem.*, 2021, **60**, 14151–14164. (d) Z.S. Dubrawski, C.Y. Chang, C.R. Carr, B.S. Gelfand, and W.E. Piers, *Dalton Trans.*, 2022, **51**, 17381–17390.
- F. Villafañe, *Coord. Chem. Rev.*, 2017, **339**, 128–137.
- (a) M. Arroyo, Á. López-Sanvicente, D. Miguel and F. Villafañe, *Eur. J. Inorg. Chem.*, 2005, 4430–4437. (b) N. Antón, M. Arroyo, P. Gómez-Iglesias, D. Miguel and F. Villafañe, *J. Organomet. Chem.*, 2008, **693**, 3074–3080. (c) P. Gómez-Iglesias, M. Arroyo, S. Bajo, C. Strohmann, D. Miguel and F. Villafañe, *Inorg. Chem.*, 2014, **53**, 12437–12448.
- (a) P. Gómez-Iglesias, F. Guyon, A. Khatyr, G. Ulrich, M. Knorr, J.M. Martín-Alvarez, D. Miguel and F. Villafañe, *Dalton Trans.*, 2015, **44**, 17516–17528. (b) E. Cuéllar, A. Diez-Varga, T. Torroba, P. Domingo-Legarda, J. Alemán, S. Cabrera, J.M.



- Martín-Alvarez, D. Miguel and F. Villafañe, *Inorg. Chem.*, 2021, **60**, 7008–7022.
- 12 P. Gómez-Iglesias, J.M. Martín-Alvarez, D. Miguel and F. Villafañe, *Dalton Trans.*, 2015, **44**, 17478–17481.
- 13 M. Arroyo, D. Miguel, F. Villafañe, S. Nieto, J. Pérez and L. Riera, *Inorg. Chem.*, 2006, **45**, 7018–7026.
- 14 M. Arroyo, P. Gómez-Iglesias, J.M. Martín-Alvarez, C.M. Alvarez, D. Miguel and F. Villafañe, *Inorg. Chem.*, 2012, **51**, 6070–6080.
- 15 Í. Ferrer, J. Rich, X. Fontrodona, M. Rodríguez and I. Romero, *Dalton Trans.*, 2013, **42**, 13461–13469.
- 16 E. Reisner, V.B. Arion, A. Ruffínska, I. Chiorescu, W.F. Schmid and B.K. Keppler, *Dalton Trans.*, 2005, **2**, 2355–2364.
- 17 (a) C.J. Jones, J.A. McCleverty and A.S. Rothin, *Dalton Trans.*, 1986, 109–111. (b) A. Romero, A. Vegas and A. Santos, *J. Organomet. Chem.*, 1986, **310**, C8–C10. (c) J. López, A. Santos, A. Romero and A.M. Echavarren, *J. Organomet. Chem.*, 1993, **443**, 221–228. (d) M.R. Kollipara, P. Sarkhel, S. Chakraborty and R. Lalrempuia, *J. Coord. Chem.*, 2003, **56**, 1085–1091. (e) P. Govindaswamy, Y.A. Mozharivskiy and M.R. Kollipara, *J. Organomet. Chem.*, 2004, **689**, 3265–3274.
- 18 (a) A.G. Jeffrey, in *An Introduction to Hydrogen Bonding*, Oxford University Press: New York, 1997. (b) T. Steiner, *Angew. Chem. Int. Ed. Eng.*, 2002, **41**, 48–76.
- 19 G. Gritzner and J. Kuta, *Pure Appl. Chem.*, 1984, **56**, 461–466.
- 20 A.H.S. Idehara, P.D.S. Gois, H. Fernandez, B.E. Goi, A.E.H. Machado, B.S. Lima-Neto and V.P. Carvalho Jr, *Mol. Catal.*, 2018, **448**, 135–143.
- 21 (a) A. Tomita and M. Sano, *Inorg. Chem.*, 1994, **33**, 5825–5830. (b) A. Tomita and M. Sano, *Inorg. Chem.*, 2000, **39**, 200–205. (c) C. Sens, M. Rodríguez, I. Romero, A. Lobet, T. Parella, B.P. Sullivan and J. Benet-Buchholz, *Inorg. Chem.*, 2003, **42**, 2040–2048. (d) J.J. Rack, A.A. Rachford and A.M. Shelker, *Inorg. Chem.*, 2003, **42**, 7357–7359.
- 22 E. Cuéllar, L. Pastor, G. García-Herbosa, J. Nganga, A.M. Angeles-Boza, A. Diez-Varga, T. Torroba, J.M. Martín-Alvarez, D. Miguel and F. Villafañe, *Inorg. Chem.*, 2021, **60**, 692–704.
- 23 B. Merillas, E. Cuéllar, A. Diez-Varga, T. Torroba, G. García-Herbosa, S. Fernández, J. Lloret-Fillol, J.M. Martín-Alvarez, D. Miguel and F. Villafañe, *Inorg. Chem.* 2020, **59**, 11152–11165.
- 24 (a) P. S. Campbell, M.H.G. Precht, C.C. Santini and P.-H. Haumesser, *Curr. Org. Chem.*, 2013, **17**, 414–429. (b) Y. Na, S. Park, S. B. Han, H. Han, S. Ko and S. Chang, *J. Am. Chem. Soc.*, 2004, **126**, 250–258.
- 25 (a) J.M. Kelly, C.M. O'Connell and J.G. Vos, *J. Chem. Soc., Dalton Trans.*, 1986, 253–258. (b) M.-N. Collomb-Dunand-Sauthier, A. Deronzier and R. Ziessel, *J. Organomet. Chem.*, 1993, **444**, 191–198. (c) E. Eskelinen, M. Haukka, T. Venäläinen, T.A. Pakkanen, M. Wasberg, S. Chardon-Noblat and A. Deronzier, *Organometallics*, 2000, **19**, 163–169. (c) A. Gabriëlsson, S. Zálíš, P. Matousek, M. Towrie and A. Viček Jr, *Inorg. Chem.*, 2004, **43**, 7380–7388.
- 26 P.L. Cheung, C.W. Machan, A.Y.S. Malkhasian, J. Agarwal and C.P. Kubiak, *Inorg. Chem.*, 2016, **55**, 3192–3198.
- 27 C.E. McCusker and J.K. McCusker, *Inorg. Chem.*, 2011, **50**, 1656–1669.
- 28 (a) A. Gennaro, A.A. Isse and E. Vianello, *J. Electroanal. Chem. Interfacial Electrochem.*, 1990, **289**, 203–215. (b) E. Fujita, C. Creutz, N. Sutin and D.J. Szalda, *J. Am. Chem. Soc.*, 1991, **113**, 343–353.
- 29 O.V. Dolomanov, L.J. Bourhis, R.J.; Gildea, J.A.K. Howard and H. Puschmann, *J. Appl. Crystallogr.*, 2009, **42**, 339–341.
- 30 G.M. Sheldrick, *Acta Crystallogr. C.*, 2015, **71**, 3–8.
- 31 G.M. Sheldrick, *Acta Crystallogr. A.*, 2008, **64**, 112–122.
- 32 (a) M. Nardelli, *Comput. Chem.*, 1983, **7**, 95–98. (b) M. Nardelli, *J. Appl. Crystallogr.*, 1995, **28**, 659–659.
- 33 (a) G.A. Jeffrey and L. Lewis, *Carbohydr. Res.*, 1978, **60**, 179–182. (b) R. Taylor and O. Kennard, *Acta Crystallogr. B.*, 1983, **39**, 133–138.